Available online at www.sciencedirect.com
ScienceDirect
Ceramics International 36 (2010) 673–678
CERAMICS INTERNATIONAL
www.elsevier.com/locate/ceramint

Fabrication and properties of porous mullite ceramics from calcined carbonaceous kaolin and α-Al_2O_3

Jiahai Bai *

School of Materials Science and Engineering, Shandong University of Technology, No. 12 Zhangzhou Road, 255049, Zibo, Shandong, PR China

Received 28 May 2009; received in revised form 11 June 2009; accepted 30 September 2009
Available online 4 November 2009

Abstract

High purity calcined carbonaceous kaolin and α-Al_2O_3 powders were employed to prepare porous mullite ceramics (Sample A) using graphite as pore former with the reaction sintering method. For the purpose of comparison, porous mullite ceramics (Sample B) was also fabricated from the uncalcined carbonaceous clay incorporated with α-Al_2O_3 powders. Mullitization in the two samples was both nearly complete at 1500 °C, despite the fact that calcination of the clay remarkably depressed mullitization and promoted the formation of glass phase. The Sample A sintered at 1500 °C fractured mainly in an intergranular way, while the Sample B mainly underwent transgranular fracture. The experimental results revealed that densification behavior/open porosity of the Sample A was far more sensitive to sintering temperature. The pore size of the Sample A as well as the Sample B sintered at 1500 °C was in a narrower range of 0.3–5 μm.

Keywords: Mullite; Porous ceramics; Carbonaceous kaolin; Fracture behavior

1. Introduction

In recent decades, porous ceramics has attracted increasing attention for its successful applications in many industry areas, such as supports for catalysts and membranes [1], filters for hot gas [2], heat exchangers for turbine engines and filters for some molten metals [3]. Mullite is one of the most important candidate materials for porous ceramics due to its high strength, low thermal expansion, high thermal shock resistance, high refractoriness and good creep resistance [4,5]. Porous mullite ceramics has been prepared from many chemical compounds, e.g. SiC and Al_2O_3, SiO_2 and Al_2O_3 or their precursors [6–8]. However, kaolin is still a preferred raw material for porous/dense mullite ceramics for much less cost [9]. Various kaolinite clays have been employed to prepare porous mullite ceramics [10–15]. For example, China clay was used to fabricate porous mullite ceramics for membrane supports with an in situ reaction sintering method [13]. Esharghawi et al. produced porous mullite ceramics from kaolin by adding Al and Mg powders [14]. Abe et al. successfully prepared bimodal porous mullite ceramics by leaching the glass matrix of the calcined body of kaolin and transition metal oxide systems [15]. In this work, a carbonaceous kaolinite clay, which contained considerable amorphous carbon and organic materials [16], was employed to fabricate porous mullite ceramics with addition of alumina. Carbonaceous kaolin is abundant in northern China, especially in Shanxi province, which is usually of high purity and widely used in glaze and refractory industries. The carbonaceous kaolin employed in this work was calcined at 1000 °C and then used to prepare mullite ceramics, as bodies containing the clay and Al_2O_3 powders for porous/dense mullite ceramics were prone to crack during the course of heating up. For the purpose of comparison, porous ceramics from the uncalcined clay was also fabricated. Phase evolution, fracture surface microstructures, open porosity, firing shrinkage and pore size distribution of the two samples were compared.

2. Experimental procedure

2.1. Materials and specimen preparation

Carbonaceous kaolinite clay (Shanxi province, China) and α-Al_2O_3 powders (99.9%) were used as starting materials and

* Tel.: +86 533 2788510; fax: +86 533 2786998.
E-mail address: zbbjh@sdut.edu.cn.

0272-8842/$36.00
doi:10.1016/j.ceramint.2009.10.006

Table 1
Chemical composition of the carbonaceous clay used in this work.

Component (wt.%)								
SiO_2	Al_2O_3	MgO	CaO	Fe_2O_3	K_2O	Na_2O	TiO_2	IOL
42.43	35.97	0.16	0.52	0.25	0.20	0.20	0.47	19.81

graphite powders (99.0%) as pore former. The chemical composition of the clay was listed in Table 1. The average particle size of the clay and Al_2O_3 powders was 3.05 μm and 0.5 μm, respectively. The carbonaceous kaolin was calcined at 1000 °C for 2 h. The weight ratio of the calcined clay to Al_2O_3 powders was determined according to chemical stoichiometry of mullite. Additional 15 wt.% graphite (99.0%) with the medium size of 10 μm was added as pore former. The clay, Al_2O_3 powders and graphite were mixed for 2 h in a high energy planetary ball mill using zirconia balls as media at a rotation speed of 250 rpm. After being dried at 110 °C in an oven, mixed with certain binder (PVA) in a mortar and sieved through a 40-mesh screen, the powders were bidirectionally pressed into rectangular specimens of 5.0 mm × 10.0 mm × 50.0 mm under the pressure of 20 MPa using a steel die. The specimens were heated to burning out graphite before 900 °C at a heating rate of 2 °C/min and then heated up to 1400 °C, 1450 °C, 1500 °C or 1550 °C in air at a heating rate of 5 °C/min. The soaked time at peak temperatures was 4 h. For the purpose of comparison, porous mullite ceramics was also prepared from the uncalcined clay and Al_2O_3 powders under the similar experimental conditions. Thereafter, the ceramics prepared from the calcined clay and the uncalcined clay was referred to Samples A and B, respectively.

2.2. Characterization

The differential thermal analysis and thermo-gravimetry (TG–DTA) of the kaolin powders were examined in flowing air by a thermal analyzer (NETZSCH STA 449 C) with α-Al_2O_3 as the reference material at a heating speed of 10 °C/min. The crystal phases of the carbonaceous kaolin, calcined kaolin and the as-prepared ceramics were identified by X-ray diffraction (XRD) analysis using a diffractometer (D8 Advance, Brucker, Germany), equipped with a Ni-filtered Cu Kα radiation source (λ = 0.154178 nm). The microstructures of fracture surfaces of the sintered specimens and morphology of mullite were observed with a field emission scanning electron microscope (FESEM, Sirion 2000, FEI, Netherlands). Linear firing shrinkage was simply calculated by measuring the length of the specimens before and after sintering. Bulk density and open porosity were determined by the Archimedes method using distilled water as liquid media. Pore size distribution was determined with mercury porosimetry (PM-60GT, Quantachrome, America). Flexural strength was tested via a three-point bending test (ATOGRAPH AG-I, Shimadzu) with a support distance of 40.0 mm and a cross-head speed of 0.50 mm/min.

3. Results and discussion

Fig. 1 showed the TG–DTA curves of the carbonaceous clay. As shown in Fig. 1, there were two distinct weight loss processes. The first weight loss was due to the evaporation of absorbed water. The second weight loss was far greater, up to 19.32 wt.%, in the temperature range about from 300 °C to 900 °C. Not as expected, the characteristic endothermic peak due to the hydration of kaolinite was not present. Instead, there were two exothermic peaks occurring at 333.4 °C and 471.7 °C, respectively, which were attributed to the oxidation of organic materials and amorphous carbon contained in the clay. It was assumed that the oxidation and removal of the amorphous carbon from the kaolin were mainly responsible for the absence of characteristic endothermic peak of kaolinite. Another exothermic peak at 1000.4 °C was due to the formation of spinel or γ-Al_2O_3 and amorphous silica [17–21]. Moreover, another exothermic peak at about 1300 °C was observed, which may be due to the mullitization of SiO_2 and Al_2O_3.

Fig. 2 showed the XRD patterns of the carbonaceous kaolin and the 1000 °C calcined kaolin. It can be seen from Fig. 2 that kaolinite was the only appreciable crystal phase, which can be confirmed by its chemical composition listed in Table 1, where the Al_2O_3/SiO_2 molar ratio was 0.499, nearly equal to that of kaolinite. When calcined at 1000 °C for 2 h, the kaolin was transformed to a mixture of γ-Al_2O_3, amorphous silica, mullite, quartz and metakaolinite. However, the amount of the mullite or quartz was far less. Fig. 3(a) presented the XRD patterns of the Samples A and B sintered at 1400, 1450, 1500 and 1550 °C, respectively. As shown in Fig. 3(a), there were no evident peaks of α-Al_2O_3 in the both samples sintered at 1500 °C or 1550 °C. Moreover, no remarkable changes occurred in the XRD patterns when the sintering temperature was increased from 1500 °C to 1550 °C. However, the characteristic peaks of α-Al_2O_3 could be indexed in the XRD patterns of the two samples sintered at whether 1400 °C or 1450 °C despite the fact that some peaks were far weaker. Therefore, it could be concluded that the mullitization was both nearly complete at 1500 °C in the Sample A and B. Nevertheless, mullitization behaviors of the two samples were not identical. To clarify the difference in the mullitization behavior of the two samples, XRD patterns from $2\theta = 42^\circ$ to 44° was magnified and showed in Fig. 3(b).

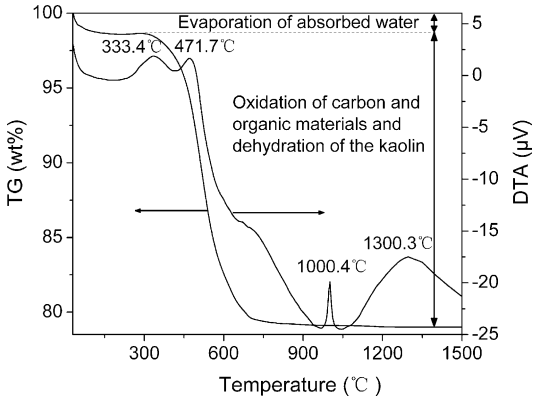

Fig. 1. TG–DTA curves of the carbonaceous kaolin.

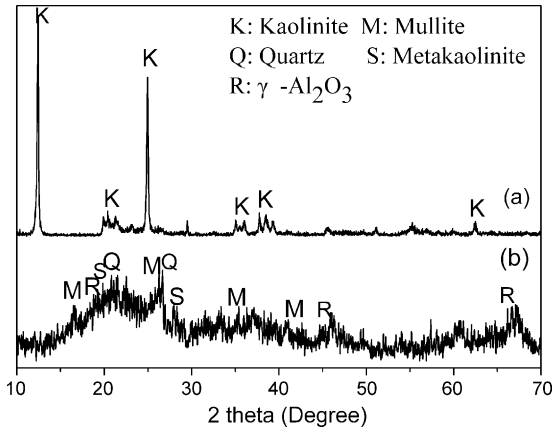

Fig. 2. XRD patterns of (a) the carbonaceous kaolin and (b) the kaolin calcined at 1000 °C for 2 h.

The ratio (*R*-value) of the intensity of α-Al_2O_3 at $2\theta = 43.36°$ to that of mullite at $2\theta = 42.59°$ was used to qualitatively represent the relative amount of the residual Al_2O_3 in the sintered body. Based on the Fig. 3 (b), the *R*-value of the Samples A and B sintered at 1400 °C and 1450 °C was 0.799 and 0.717, 0.188 and 0.130, respectively, disclosing that there are more residual α-Al_2O_3 and less mullite in the Sample A and that mullitization in the Sample A was remarkably hindered by the calcination of the carbonaceous kaolin. Based on the *R*-value, it was also inferred that the increment in the relative content of mullite of the Sample A was much more than that of the Sample B when the sintering temperature was increased from 1400 °C to 1450 °C. XRD analysis also revealed that no appreciable characteristic peak of quartz was detected in the two samples sintered at 1400 °C or 1450 °C. For the weight ratios of SiO_2 to Al_2O_3 in the two samples were (nearly) equal to the chemical stoichiometry of mullite, there should be some glassy SiO_2 in the two samples, which was related to the liquid phase formed by some SiO_2 and certain Al_2O_3 at higher temperatures no lower than 1260 °C [22,23]. For more residual α-Al_2O_3 occurred in the Sample A, it was believed that more glass phase was formed in it, revealing that more liquid phase appeared in the Sample A at the sintering temperatures.

Fig. 4 showed the FESEM micrographs of the Samples A and B sintered at 1500 °C. Two different microstructures were observed on the fracture surfaces of Sample A or B. One was the micro-areas which were subject to fracture and formed by cracking as shown in Fig. 4(a1) or (b1), the other was some inherent micro-areas which did not undergo cracking as presented in Fig. 4(a2) or (b2). As shown in Fig. 4(a1), considerable surfaces of fractured spots were smoother and the shape of the needle-like mullite could be deduced based on the morphology of the fractured spot surfaces. On the other hand, most fractured spot surfaces presented in Fig. 4 (b1) were much rougher and more irregular. Therefore, it could be concluded that the Sample A from the calcined kaolin fractured mainly in an intergranular manner, while the Sample B mainly underwent transgranular fracture. It can be seen from Fig. 4(a2) and (b2) that the needle-like mullite crystals were bimodal in size, i.e. larger primary mullite and smaller secondary mullite crystals.

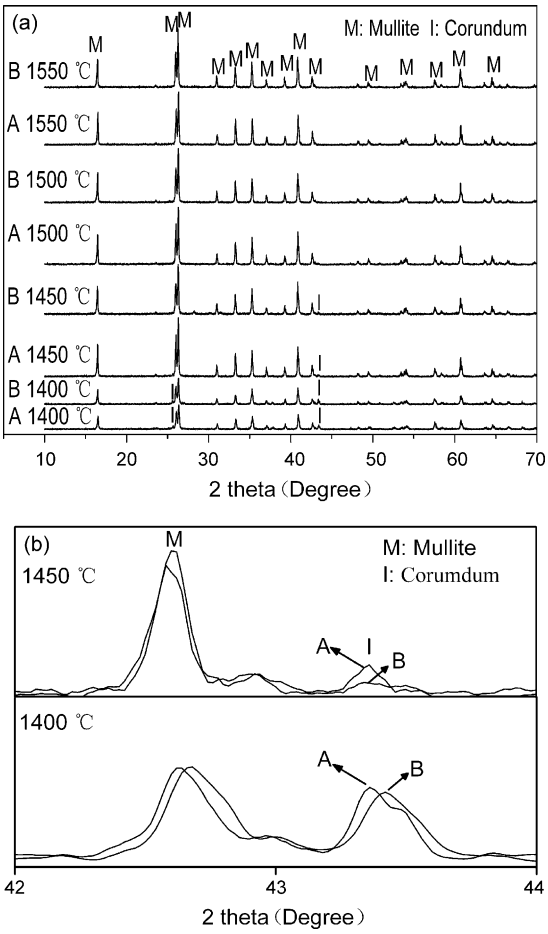

Fig. 3. XRD patterns (a) of the Samples A and B sintered at 1400 °C, 1450 °C, 1500 °C and 1550 °C, respectively, and the magnified XRD patterns (b) in the range of $2\theta = 42–44°$ of the Samples A and B sintered at 1400 °C and 1450 °C, repetitively. Sample A: from the calcined kaolin, Sample B: from the carbonaceous kaolin.

Nevertheless, the relative content of secondary mullite crystals in the Sample A appeared much more than that in the Sample B. Moreover, there appeared more vitreous luster in the Sample A than B, revealing more glass phase was formed in the former. Therefore, it could be inferred that the fracture behaviors of the two samples were related to the glass phase as there was no another phase presented in the two samples. More glass phase formed in the Sample A could make the mullite crystals bonded enough and thus led to the intergranular fracture, while the glass phase in the Sample B was not enough for bonding of the mullite crystals and thus it fractured mainly in the transgranular manner. Furthermore, more glass phase in the Sample A implied that less mullite was formed, disclosing that calcination of the clay remarkably depressed the formation of mullite, in good agreement with the result obtained from XRD analysis. It also implied that more liquid phase occurred in the Sample A when it was being sintered at 1500 °C, which was, at least partly, responsible for the fact that relatively more second mullite crystals were formed in the Sample A.

Fig. 5 represented open porosity and bulk density of the mullite ceramics as functions of the sintering temperatures prepared from the uncalcined clay and the calcined clay,

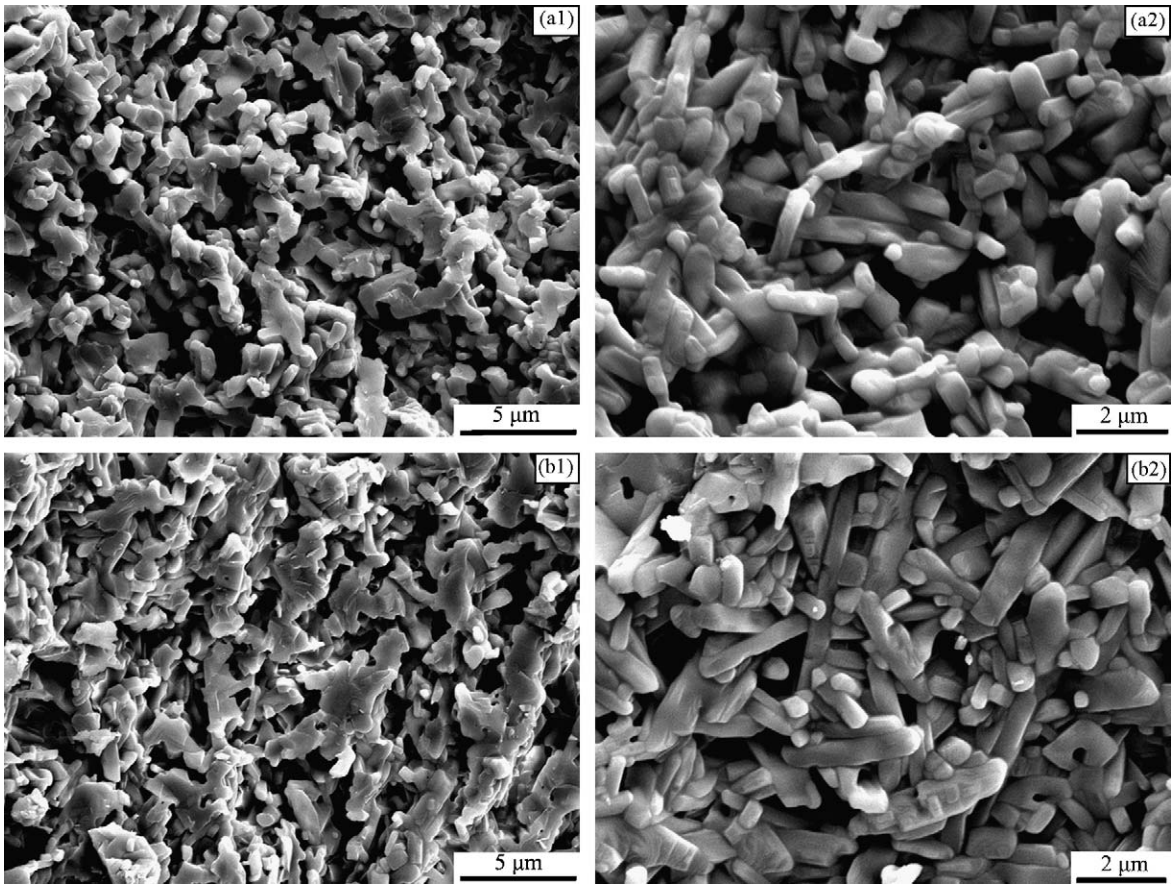

Fig. 4. FESEM micrographs of fracture surfaces of the Samples A and B calcined at 1500 °C. (a1, a2): The Sample A from the calcined kaolin. (b1, b2): The Sample B from the carbonaceous kaolin.

respectively. As shown in Fig. 5, the open porosity of the two samples first increased slightly when the sintering temperature was raised from 1400 °C to 1450 °C and then decreased sharply with further increasing of sintering temperature. It is interesting that the open porosity of the Sample A decreased more than that of the Sample B with increasing of the sintering temperature from 1400 °C to 1450 °C. Compared with Sample B, the open porosity of Sample A was much higher when the samples were sintered at 1400 °C or 1450 °C, while it was decreased dramatically and become lower as sintering temperature further rose to 1550 °C. So it was concluded that the densification of the Sample A was more sensitive to sintering temperature than the Sample B. For the bulk density, it went in the opposite way to open porosity. The differences in open porosity/bulk density between the Sample A and B can be confirmed by the firing shrinkage presented in Fig. 6, which changed in the same manner as bulk density, i.e. the firing shrinkage of the Sample A

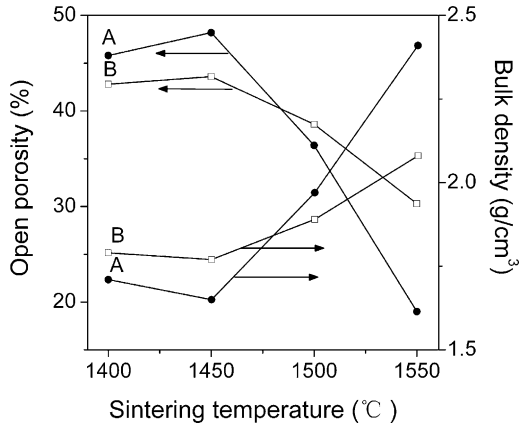

Fig. 5. Open porosity and bulk density of the Samples A and B as functions of the sintering temperatures. Sample A: from the calcined kaolin. Sample B: from the uncalcined carbonaceous kaolin.

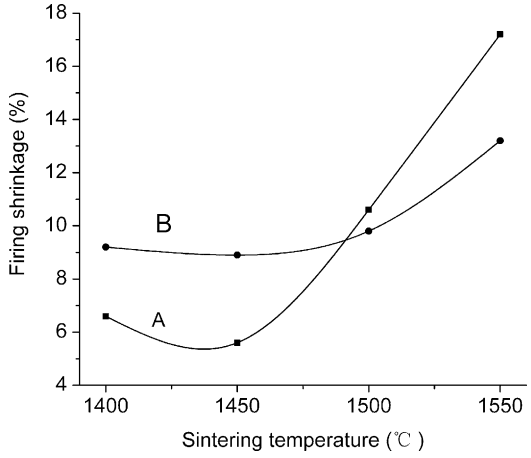

Fig. 6. Firing shrinkage of Samples A and B as functions of the sintering temperatures. Sample A: from the calcined kaolin. Sample B: from the uncalcined carbonaceous kaolin.

first fell slightly but much more and then rose more sharply with increasing of the sintering temperatures as compared with the Sample B.

The difference in the densification behavior between Samples A and B were mainly related to the dehydration of kaolinite, mullite formation and the liquid phase which mainly derived from SiO_2 and Al_2O_3 at higher temperatures. To investigate the effect of the dehydration of kaolinite on linear shrinkage, the Samples A and B were both heat treated at 800 °C for 2 h. About 4% linear shrinkage occurred in the Sample B, while no appreciable shrinkage in the Sample A. Therefore, the dehydration of kaolinite could make a significant contribution to densification. So the Sample B exhibited less open porosity than the Sample A when they were sintered at 1400 °C or 1450 °C, though more liquid phase was formed in the Sample A. At the same time, when the sintering temperature was increased from 1400 °C to 1450 °C, more increment in the relative content of mullite took place in the Sample A than B, i.e. more increment in volume expansion occurred in the former, which was attributed to the fact that mullitization of SiO_2 and Al_2O_3 usually leads to a significant volume expansion due to the difference in density amongst mullite, SiO_2 and Al_2O_3 [5], so open porosity of the Sample A fell more. When the sintering temperature was elevated to 1500 °C or 1550 °C, it could be inferred that there was much more liquid in the Sample A based on the above discussion, so densification of the Sample A became much more remarkable and its open porosity became remarkably less as compared with the Sample B.

For higher sintering temperature led to far less porosity and the mullitizaion was nearly completed at 1500 °C, it was believed that 1500 °C was an optimal sintering temperature for the porous mullite ceramics prepared in the present work. Noting that the open porosity and bulk density of the Sample A sintered at 1500 °C was 36.4% and 1.97 g/cm^3, respectively.

Fig. 7 showed the pore size distribution of the Samples A and B sintered at 1500 °C. As shown in Fig. 7, the pore size of the two samples was both mainly in a narrower range of 0.3–5 μm. On the other hand, the average pore size of the Sample A was slightly smaller than that of the Sample B, which could be attributed to the fact that more densification occurred in the Sample A.

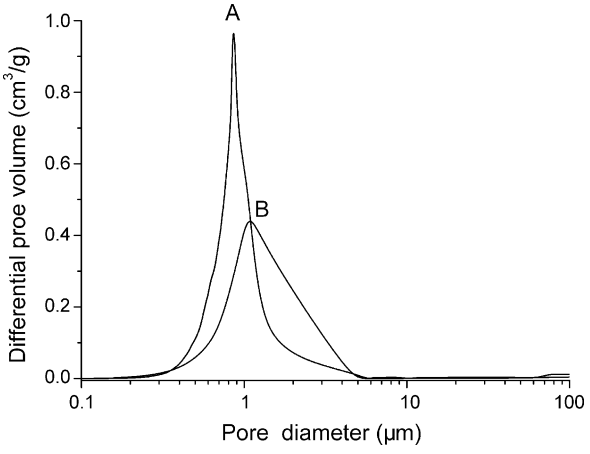

Fig. 7. Pore size distribution of the two samples. Sample A: from the calcined kaolin. Sample B: from the uncalcined carbonaceous kaolin.

Finally, it was worth noting that the flexural strength of the Sample A sintered at 1500 °C and 1550 °C was 42.1 MPa and 75.9 MPa, respectively. However, no crack-free porous ceramics was prepared from the uncalcined kaolin under the experimental conditions used in this work, thus no data on flexural strength of the Sample B could be given.

4. Conclusions

Porous mullite ceramics was successfully fabricated from high purity calcined carbonaceous kaolin and α-Al_2O_3 powders using graphite as pore former. Open porosity, flexural strength of the porous ceramics sintered at 1500 °C was 36.4% and 42.1 MPa, respectively. Its pore size was in a narrower range of 0.3–5 μm.

Compared with the Sample B, the densification behavior of the Sample A was far more sensitive to the sintering temperatures. Its open porosity rose slightly but more when sintering temperature was increased from 1400 °C to 1450 °C, then fell more sharply with further increasing of the sintering temperatures.

Mullitization of the Samples A and B was both nearly complete at 1500 °C. Nevertheless, the mullite formation in the former was depressed remarkably by calcination of the clay at 1000 °C for 2 h, as compared with the Sample B.

The Sample A sintered at 1500 °C fractured mainly in an intergranular way, while the Sample B mainly underwent transgranular fracture.

References

[1] Z.R. Ismagilov, R.A. Shkrabina, N.A. Koryabkina, A.A. Kirchanov, et al., Porous alumina as a support for catalysts and membranes. Preparation and study, React. Kinet. Catal. Lett. 60 (2) (1997) 225–231.
[2] Y.M. Jo, R.B. Hutchison, J.A. Raper, Characterization of ceramic composite membrane filters for hot gas cleaning, Powder Technol. 91 (1) (1997) 55–62.
[3] P.M. Then, P. Day, The catalytic converter ceramic substrate—an astonishing and enduring invention, Interceramics 49 (1) (2000) 20–23.
[4] H. Schneider, E. Eberhard, Thermal expansion of mullite, J. Am. Ceram. Soc. 73 (7) (1990) 2073–2076.
[5] Y.F. Chen, M.C. Wang, M.H. Hon, Phase transformation and growth of mullite in kaolin ceramics, J. Eur. Ceram. Soc. 24 (2004) 2389–2397.
[6] S.Q. Ding, Y.P. Zeng, D.L. Jiang, Fabrication of mullite ceramics with ultra high porosity by gel freeze drying, J. Am. Ceram. Soc. 90 (7) (2007) 2276–2279.
[7] J.H. She, T. Ohji, Porous mullite ceramics with high strength, J. Mater. Sci. Lett. 21 (2002) 1833–1834.
[8] k. Okada, N. Otsuka, Review of mullite synthesis routes in Japan, Am. Ceram. Soc. Bull. 70 (1971) 1633–1640.
[9] I. Ganesh, J.M.F. Ferreira, Influence of raw material type and of the overall chemical composition on phase formation and sintered microstructure of mullite aggregates, Ceram. Int. (2009), doi:10.1016/j.ceramint.2008.11.008.
[10] Y.F. Liu, X.Q. Liu, H. Wei, G.Y. Meng, Porous mullite ceramics from national clay produced by gel casting, Ceram. Int. 27 (1) (2001) 1–7.
[11] J. Pascual, J. Zapatero, M.C.J. de Haro, I. Varona, et al., Porous mullite and mullite-based composites by chemical processing of kaolinite and aluminum metal wastes, J. Mater. Chem. 10 (6) (2000) 1409–1414.

[12] J. Pascual, J. Zapatero, M.C.J. de Haro, A.J.R. del Valle, et al., Preparation of mullite ceramics from coprecipitated aluminum hydroxide and kaolinite using hexamethylenediamine, J. Am. Ceram. Soc. 83 (11) (2000) 2677–2680.
[13] G.L. Chen, H. Qi, W.H. Xing, N.P. Xu, et al., Direct preparation of macroporous mullite supports for membranes by in situ reaction sintering, J. Membr. Sci. 318 (2008) 38–44.
[14] A. Esharghawi, C. Penot, F. Nardou, Contribution to porous mullite synthesis from clays by adding Al and Mg powders, J. Eur. Ceram. Soc. 29 (1) (2009) 31–38.
[15] H. Abe, H. Seki, A. Fukunaga, M. Egashira, Preparation of bimodal porous mullite ceramics, J. Mater. Sci. 29 (5) (1994) 1222–1226.
[16] M. Zhao, S.T. Li, H.S. Qin, C.S. Zhu, Structure and characteristics of modified coal shale filler used as NR fillings (in Chinese), Acta Miner. Sin. 26 (2006) 113–117.
[17] W.M. Carty, U. Senapati, Porcelain—raw materials, processing, phase evolution, and mechanical behavior, J. Am. Ceram. Soc. 81 (1998) 3–20.
[18] G.W. Brindley, M. Nakahira, The kaolinite–mullite reaction series. III. The high-temperature phases, J. Am. Ceram. Soc. 42 (1959) 319–323.
[19] G.W. Brindley, M. Nakahira, Kinetics of dehydroxylation of kaolinite and halloysite, J. Am. Ceram. Soc. 40 (1957) 346–350.
[20] K.C. Liu, G. Thomas, Time–temperature–transformation curves for kaolinite–alumina, J. Am. Ceram. Soc. 77 (1994) 545–552.
[21] C.Y. Chen, G.S. Lan, W.H. Tuan, Microstructural evolution of mullite during the sintering of kaolin powder compacts, Ceram. Int. 26 (2000) 715–720.
[22] R.F. Davis, J.A. Pask, Diffusion and reaction studies in the system Al_2O_3–SiO_2, J. Am. Ceram. Soc. 55 (1972) 525–528.
[23] K.C. Liu, G. Thomas, A. Caballero, J.S. Moya, et al., Mullite formation in kaolinite–α-alumina, Acta Metall. Mater. 42 (2) (1994) 489–495.